POLITECNICO DI TORINO
Repository ISTITUZIONALE

Structure-Dependent Influence of Moisture on Resistive Switching Behavior of ZnO Thin Films

Original
Structure-Dependent Influence of Moisture on Resistive Switching Behavior of ZnO Thin Films / Milano, G.; Luebben, M.; Laurenti, M.; Boarino, L.; Ricciardi, C.; Valov, I.. - In: ADVANCED MATERIALS INTERFACES. - ISSN 2196-7350. - ELETTRONICO. - 8:16(2021), p. 2100915. [10.1002/admi.202100915]

Availability:
This version is available at: 11583/2936401 since: 2021-11-09T10:24:44Z

Publisher:
John Wiley and Sons Inc

Published
DOI:10.1002/admi.202100915

Terms of use:
openAccess

This article is made available under terms and conditions as specified in the corresponding bibliographic description in the repository

Publisher copyright

(Article begins on next page)

16 July 2022

ADVANCED MATERIALS INTERFACES
www.advmatinterfaces.de

Structure-Dependent Influence of Moisture on Resistive Switching Behavior of ZnO Thin Films

Gianluca Milano, Michael Luebben, Marco Laurenti, Luca Boarino, Carlo Ricciardi,* and Ilia Valov**

Resistive switching mechanisms underlying memristive devices are widely investigated, and the importance as well as influence of ambient conditions on the electrical performances of memristive cells are already recognized. However, detailed understanding of the ambient effect on the switching mechanism still remains a challenge. This work presents an experimental investigation on the effect of moisture on resistive switching performances of ZnO-based electrochemical metallization memory cells. ZnO thin films are grown by chemical vapor deposition (CVD) and radio frequency sputtering. Water molecules are observed to influence electrical resistance of ZnO by affecting the electronic conduction mechanism and by providing additional species for ionic conduction. By influencing dissolution and migration of ionic species underlying resistive switching events, moisture is reported to tune resistive switching parameters. In particular, the presence of H_2O is responsible for a decrease of the forming and SET voltages and an increase of the ON/OFF resistance ratio in both CVD and sputtered films. The effect of moisture on resistive switching performance is found to be more pronounced in case of sputtered films where the reduced grain size is responsible for an increased adsorption of water molecules and an increased amount of possible pathways for ion migration.

G. Milano, L. Boarino
Advanced Materials Metrology and Life Sciences Division
Istituto Nazionale di Ricerca Metrologica (INRiM)
Strada delle Cacce 91, Torino 10135, Italy
E-mail: g.milano@inrim.it

M. Luebben, I. Valov
Institute for Materials in Electrical Engineering II
RWTH Aachen University
Sommerfeldstrasse 24, 52074 Aachen, Germany
E-mail: i.valov@fz-juelich.de

M. Luebben, I. Valov
JARA – Fundamentals for Future Information Technology
52425 Jülich, Germany

M. Laurenti, C. Ricciardi
Department of Applied Science and Technology
Politecnico di Torino
C.so Duca degli Abruzzi 24, Torino 10129, Italy
E-mail: carlo.ricciardi@polito.it

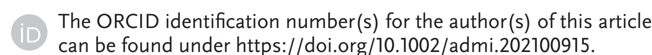
The ORCID identification number(s) for the author(s) of this article can be found under https://doi.org/10.1002/admi.202100915.

© 2021 The Authors. Advanced Materials Interfaces published by Wiley-VCH GmbH. This is an open access article under the terms of the Creative Commons Attribution License, which permits use, distribution and reproduction in any medium, provided the original work is properly cited.

DOI: 10.1002/admi.202100915

1. Introduction

Two-terminal memristive devices relying on resistive switching phenomena in metal-insulator-metal structured devices have recently attracted great attention for the realization of next-generation memories and neuromorphic architectures.[1–4] In case of devices based on the electrochemical metallization memory (ECM) effect, the physical mechanism of switching relies on electrochemical effects and nanoionic processes involving dissolution of metal atoms from an electrochemically active electrode and consequent migration of metal ions in an insulating matrix to form a metallic conductive bridge that is responsible for the change of the device resistance.[5,6] Previous reports showed that resistive switching mechanism is strongly influenced by extrinsic effects such as the presence of moisture that can diffuse and be adsorbed in the insulating matrix.[7,8,17,18,9–16] In particular, the influence of moisture on the functionalities of a resistive switching cell was observed to depend on the specific chemical/structural properties of the involved materials.[7] Among metal-oxides, semiconducting ZnO was widely exploited as active material for the realization of electronic devices. Thanks to its peculiar photonic, mechanical and electronic properties together with the biocompatibility and environmentally friendly characteristics, ZnO has also been considered as a promising candidate for a wide range of applications including field effect transistors, piezoelectric transducers, photovoltaics, sensors, and photodetector.[19–24] Also, the interest in ZnO is related to the possibility to be grown with a wide range of morphologies including nanowires, nanorods, nanobelts, and nanosheets.[25,26] In this framework, resistive switching phenomena were observed in a wide range of ZnO nanostructures including nanowires/nanorods,[27–29] nanoislands,[30] and in a wide range of thin films realized with different deposition techniques.[31,32,41,33–40] In particular, in the field of resistive switching devices, great interest is devoted to ZnO in fabricating devices for transparent electronics owing to its high transparency to visible light,[37–39] also taking into advantage of its radiation hardness.[42]

Even if the influence of moisture has been investigated in a wide range of metal oxides, the particular effect of moisture on resistive switching devices is material specific depending

on (electro)catalytic properties of the electrodes as well as on the involved insulating matrix.[7] In this framework, the investigation of the influence of moisture on ZnO-based thin film devices is still missing. Also, the effect of structural properties of involved thin-film-based insulating matrix on resistive switching behavior still needs to be clarified.

In this work, we investigated the structure-dependent influence of moisture on resistive switching properties of ECM cells based on ZnO thin films. In particular, thin films characterized by different structural properties realized by chemical vapor deposition (CVD) and by radiofrequency (RF) sputtering were considered. The presence of moisture was reported to influence electrical resistance as well as resistive switching parameters of ZnO-based resistive switching cells. In particular, moisture was observed to be responsible for a decrease of both forming and SET voltages and an increase of the ON/OFF ratio. The influence of H_2O is more pronounced for sputtered films where the film texture is characterized by smaller grains and, thus, a larger number of grain boundaries that are responsible for an enhanced adsorption of moisture. Furthermore, more grain boundaries with adsorbed water open more possible pathways for ion migration through the ZnO. These results provide new insights on the influence of moisture on resistive switching devices, showing that the effect of moisture depends not only on the insulating matrix material but also on its structural properties.

2. Results

To investigate the influence of moisture on resistive switching properties of ZnO films, electrical characterizations of Ag/ZnO/Pt thin film ECM cells were performed in a controlled atmosphere as schematized in **Figure 1**a. The cells with stacked structure (Figure 1b) were fabricated by depositing ZnO layers with different crystal quality. For this purpose, thin films with grain size of ≈150 nm and thickness of 320 nm were grown by CVD while ZnO layers with grain size of ≈15 nm and thickness of 40 nm were deposited by RF sputtering (Figure 1c,d, respectively). Details of the fabrication process are reported in the Experimental Section. These films are characterized by highly oriented grains resulting in a polycrystalline columnar structure as a consequence of the preferential growth of ZnO along the *c*-axis of the wurtzite structure. In particular, X-ray diffraction (XRD) analyses reported in our previous work[43] revealed that the prominent peak in the diffraction pattern is

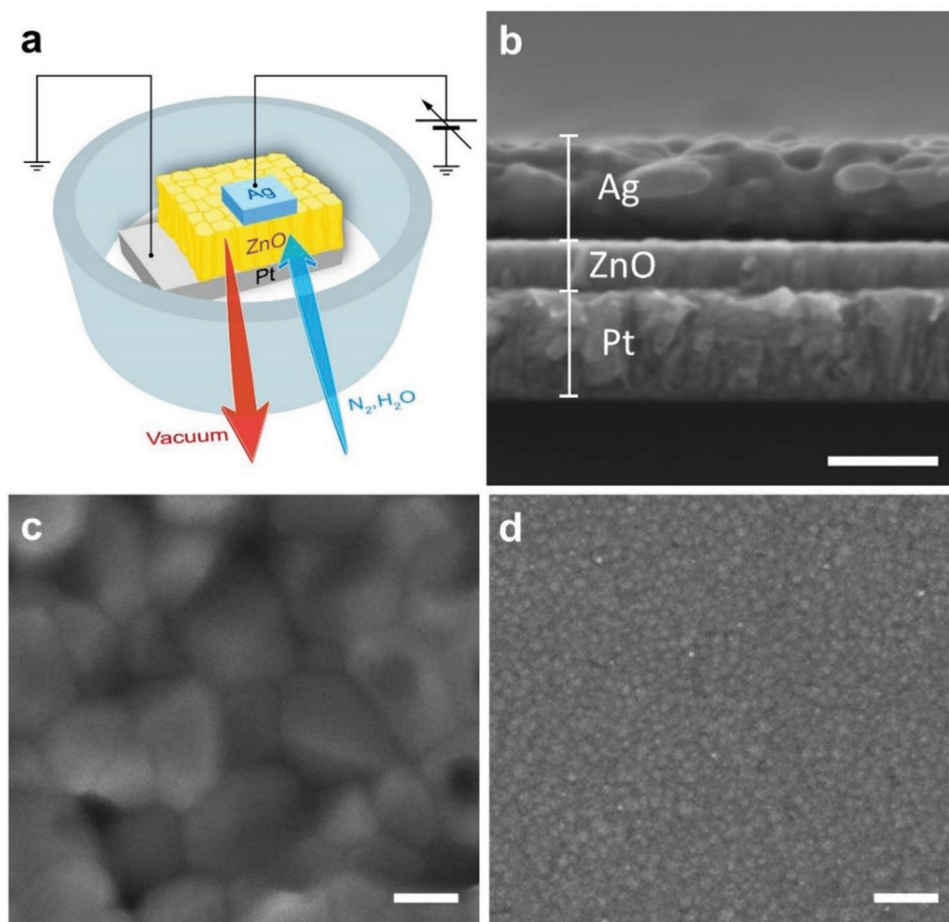

Figure 1. Atmosphere-controlled measurements and device structure. a) Schematic presentation of atmosphere-controlled electrical measurements. b) SEM cross-sectional image of a stacked resistive switching device where the ZnO thin film is sandwiched in between an Ag top electrode and a Pt bottom electrode. The image refers to a ZnO thin film realized by sputtering. SEM top view of a ZnO thin film c) by CVD with a grain size of ≈150 nm and d) by sputtering with a grain size of ≈15 nm (scale bars, 100 nm).

© 2021 The Authors. Advanced Materials Interfaces published by Wiley-VCH GmbH

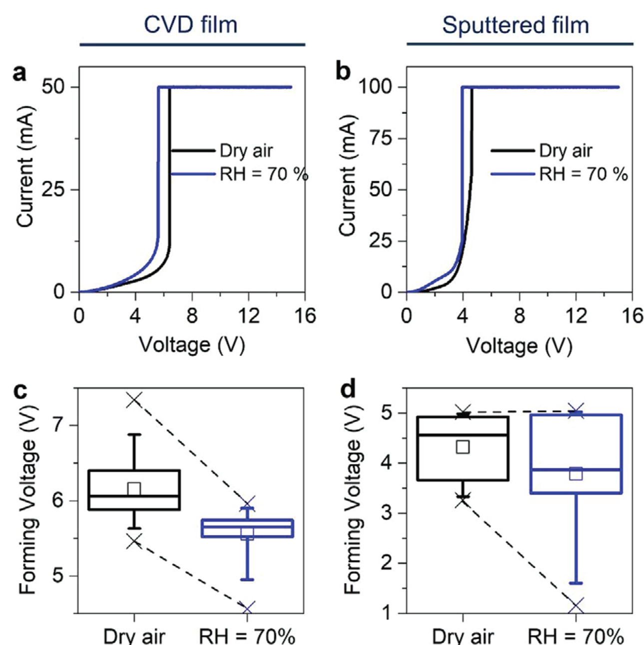

Figure 2. Influence of moisture on electroforming. Electroforming process of Ag/ZnO/Pt memristive cells based on ZnO thin films realized by a) CVD and b) sputtering in dry air and at RH = 70% in a N_2 environment. Box plots of the forming voltage in the two different environmental conditions for c) CVD and d) sputtered films. Each box plot was obtained by measuring the forming voltage in ten different devices. The dotted lines are guides to the eyes.

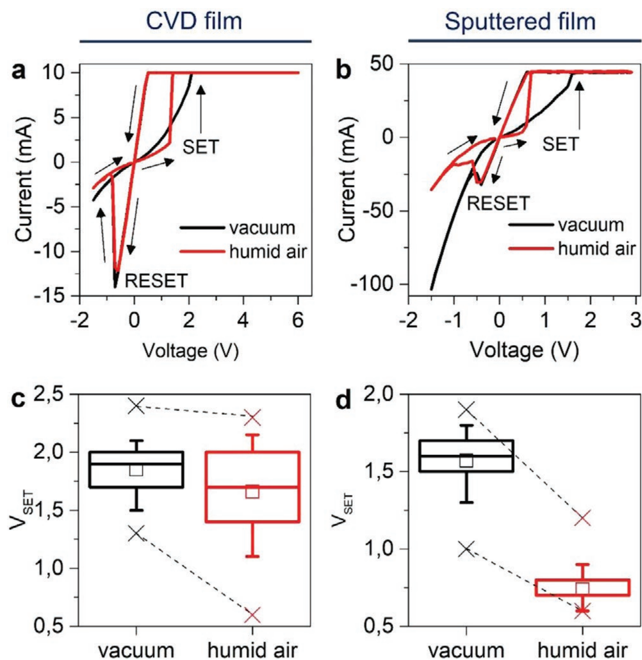

Figure 3. Influence of moisture on resistive switching behavior. Comparison of the *I–V* characteristics in humid air and in vacuum of ZnO films realized by a) CVD and b) sputtering in Ag/ZnO/Pt stacked device configuration. Box plots of the SET voltage in the two different environmental conditions for c) CVD and d) sputtered films. Box plots were obtained by measuring the SET voltage in 50 consecutive resistive switching cycles by considering the same device in the two different environmental conditions.

located at ≈34.5° and ≈34.1° for CVD and sputtered ZnO films, respectively. This peak is attributable to the diffraction of (002) ZnO planes resulting from the highly oriented grains along the *c*-axis. Also, the (002) peak was observed to be larger in case of sputtered films due to the smaller crystal size. These observations were corroborated by transmission electron microscopy (TEM) analysis and Raman spectroscopy reported in our previous work.[43]

By considering Ag/ZnO/Pt resistive switching devices, the electroforming characteristics of CVD and sputtered films are shown in **Figure 2**a,b, respectively. A slight decrease of the forming voltage occurred when the device was exposed to high levels of relative humidity (RH). The median electroforming voltage measured across different memristive cells decrease from 6.1 to 5.7 V in CVD films (Figure 2c) and from 4.6 to 3.9 V in sputtered films (Figure 2d) when passing from dry conditions (dry N_2) to RH = 70% in a N_2 environment.

The presence of humidity was also observed to impact resistive switching behavior following the forming process. The comparison of resistive switching *I–V* characteristics of CVD and sputtered films in humid air (RH ≈ 20–30%) and in vacuum is presented in **Figure 3**. A shift of the SET events toward higher voltage values were observed in vacuum in absence of moisture. A slight shift of the SET voltage was observed in CVD films where the median values of V_{SET} measured over cycling increase from 1.7 to 1.9 V passing from air to vacuum conditions (Figure 3c). Instead, a more pronounced shift of SET voltages was observed in the sputtered films where V_{SET} increased from 0.7 V in air to 1.6 V in vacuum (Figure 3d). Instead, no significant variations of RESET voltages and currents were observed for both types of ZnO (Section S1, Supporting Information).

Not only operating voltages but also resistance state values were observed to be influenced by the presence of moisture. LRS and HRS values over cycling measured in humid air and vacuum conditions of CVD memristive cells are shown in **Figure 4**a,b, respectively. It can be seen that, while no significant differences were observed in case of LRS, the HRS exhibited a significant decrease in vacuum conditions. Indeed, the median value of HRS over cycling was observed to decrease from 855 Ω in air to 534 Ω in vacuum. Since the LRS is not strongly affected by ambient conditions, the diminishing of the HRS resulted in a decrease of the HRS/LRS ratio in vacuum conditions. The median HRS/LRS ratio is decreasing from ≈20 in humid air to ≈11 in vacuum, with a decrease of ≈45% (Figure 4c). Comparable results were observed in sputtered films where the decrease of HRS was from 198 Ω in air to 72 Ω in vacuum (Figure 4d,e). Also, in this case the HRS/LRS ratio was strongly affected by humidity with a reduction of 71% in vacuum conditions, as can be seen from Figure 4f. It is worth noticing that the stability of the bipolar resistive switching behavior in sputtered ZnO was disturbed in vacuum conditions. In this case about 30% of resistive switching cycles were unstable and the device exhibited always a HRS, as shown in Figure 4e. This means that in this case the device spontaneously returns to the HRS after the SET process, resulting in an unstable switching event as discussed in Section S2 (Supporting Information).

 © 2021 The Authors. Advanced Materials Interfaces published by Wiley-VCH GmbH

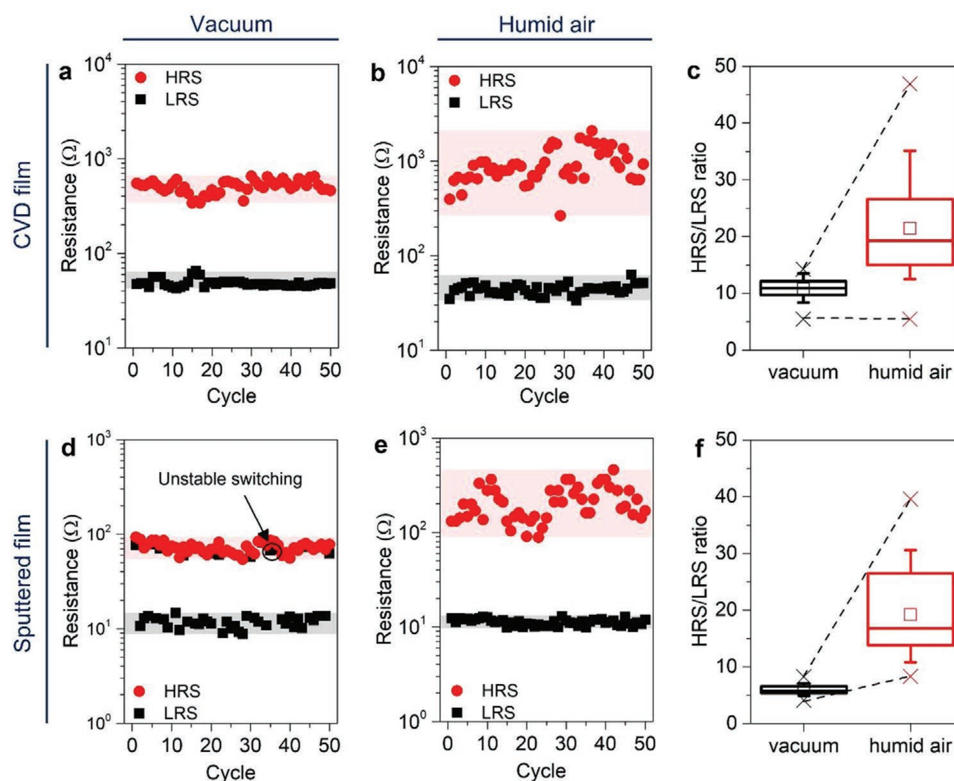

Figure 4. Influence of moisture on resistance states over cycling. HRS and LRS values over cycling of the same device based on the ZnO CVD film a) in vacuum conditions and b) in humid air with corresponding c) box plots of the HRS/LRS ratio. HRS and LRS values over cycling of the same device based on the ZnO sputtered film d) in vacuum conditions and e) in humid air with corresponding f) box plots of the HRS/LRS ratio (cycles exhibiting unstable switching in vacuum conditions were not considered in the box plots). HRS and LRS values were extrapolated from full sweep cycles at a reading voltage of 0.2 V. The dotted lines are guides to the eyes.

3. Discussion

The switching mechanism in ZnO films is attributed to dissolution of silver ions from the electrochemical active electrode with subsequent electromigration and recrystallization that leads to the formation of a conductive path in the ZnO matrix that bridges the two electrodes.[33,44,45] As a consequence of the preferred growth of ZnO films along the [002] crystallographic direction, the migration process of Ag^+ ions is facilitated by the presence of grain boundaries (GBs) that are highly oriented perpendicularly to the electrodes.[33,45] This switching mechanism in ZnO-based devices was directly investigated by Bejtka et al.[45] that reported a direct investigation of the Ag-based conductive pathway by TEM analyses. The polycrystalline structure of ZnO also influences the adsorption process of moisture as water molecules are likely to be adsorbed at ZnO GBs without penetration in the crystalline ZnO grains, as previously investigated by means of secondary ion mass spectrometry (SIMS) depth profile.[43] Based on these previous observations, the switching mechanism in ZnO films can be ascribed to dissolution and migration of Ag^+ ions along highly oriented grain boundaries where a hydrogen-bond network is present due to moisture adsorption. This represents a complex scenario where the effect of moisture is manifold, as discussed in the following.

To understand how adsorbed water impacts the electrical conductivity of the ZnO-based memristive cell, it is necessary to consider that moisture not only affects electronic transport in ZnO but provides also additional ionic species responsible for an ionic current flowing in parallel to the electronic one.[43] Concerning electronic properties, moisture adsorbed on grain boundaries is responsible for the creation of a depleted region with upward band bending on grain surfaces that results in an increase of ZnO resistance by increasing the amount of adsorbed water species. However, an opposite behavior characterized by a decreasing of resistance by increasing the moisture level can be observed due to the ionic current of protonic species flowing in parallel to the electronic one. The protonic current dominates in RF sputtered ZnO thin films where a monotonic decrease of ZnO resistance was observed while, in case of CVD films, the influence of adsorbed species on ZnO resistance dominates below RH ≈ 50% where resistance was observed to increase by increasing the moisture content and protonic current dominates for higher moisture levels where a decrease of resistance was observed by increasing RH as discussed in Section S3 (Supporting Information). It is important to remark that the relevance of the two different mechanisms of modulation of electrical conductivity of ZnO by moisture are strongly dependent on the moisture content as well as on the chemical/structural properties and treatment of the sample, as discussed in our previous work.[43] While these effects are responsible for a modulation of the ZnO electrical resistance by few percent (<5%), in the present work the effect of structure-dependent

© 2021 The Authors. Advanced Materials Interfaces published by Wiley-VCH GmbH

H_2O adsorption is shown to affect memristive device operating voltages and functionalities.

Most importantly, moisture is tuning resistive switching behavior by regulating dissolution and migration rates of Ag^+ species underlying the formation/rupture of the conductive filament. In order to understand the influence of moisture on the dissolution process, it is necessary to consider the two-terminal device as an electrochemical cell. From fundamentals of electrochemistry, an electrochemical cell can be divided in two compartments (half-cells) in which an oxidation reaction and a reduction reaction occur separately. It is important to notice that in order for the total cell reaction to proceed, both half-reactions have to take place. In the case of a memristive cell, one half-cell reaction is represented by the anodic dissolution of Ag to form Ag^+ ions at the Ag/ZnO interface, according to the oxidation reaction[28]

$$Ag \rightarrow Ag^+ + e^- \quad (1)$$

Besides this reaction, a counter electrode half-cell reaction at the Pt/ZnO interface is needed to keep electroneutrality of the cell during operation. Previous results showed that, besides electrons, OH^- species and water molecules can also play an important role in supplying the counter electrode reaction through the reduction reaction[16,46]

$$2H_2O + 2e^- \rightarrow 2OH^- + H_2 \quad (2)$$

More in general, it should be mentioned that water electrolysis at the inert electrode can result in much more complex electrochemical reactions involving also intermediate steps and products.[47] By considering the memristive cell, it is important to underline that the total cell reaction rate is determined by the slower half-cell reaction. This means that, if the device kinetic is regulated by the reduction reaction, a lower amount of residual water available for the counter electrode reaction to proceed results in a reduction of the injection rate of Ag^+ ions. In this scenario, a higher amount of moisture provides additional water species for the counter electrode reaction to proceed with consequent increase of the injection rate of Ag^+ ions. The abovementioned discussion is corroborated also by the observations of Liu et al.[48] that related the accumulation of static charges revealed by electrostatic force microscopy (EFM) measurements on ZnO films to the presence of hydroxyl species due to the reduction of moisture at the counter electrode after switching events. Also, this in in agreement with observations of Lübben et al.[46] that observed that the reaction kinetics of water splitting are limiting the overall kinetics of Ag-based ECM cells.

However, previous works revealed that moisture also has a strong impact on the Ag^+ ionic migration mechanism on ZnO crystalline surfaces.[49] Indeed, theoretical and experimental investigation revealed that water species adsorbed on a crystalline ZnO surface (here represented by grain surfaces) are responsible for a decrease of the diffusion barrier of Ag^+ ions, facilitating the formation of the metallic filament underlying resistive switching events. The lowering of the diffusion barrier was shown to be related to a qualitative change of the diffusion mechanism of silver ions that, in presence of moisture, move

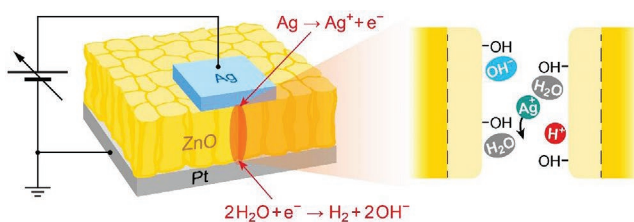

Figure 5. Influence of moisture on resistive switching behavior of ZnO thin films. Moisture that is adsorbed at ZnO grain boundaries regulates dissolution of Ag^+ species participating in the counter electrode reaction and affects the ionic migration mechanism along grain boundaries where a hydrogen-bond network and water molecules are present. In addition, moisture is a source of protonic species that contributes to the global electrical conductivity of ZnO.

from one water molecule to the next one by forming Ag—OH complexes that prevent their interaction with Zn atoms on the surface.[49]

The above discussed mechanisms (schematized in **Figure 5**) can explain the observed changes of resistive switching behavior of ZnO thin films. Promoting dissolution and migration of Ag^+ ions, moisture is responsible for lowering the energy required for the formation of a conductive path, reducing both forming and SET voltages and causing more abrupt SET events as observed experimentally (Figures 2 and 3). Similarly, the larger ON/OFF ratio observed in presence of moisture (Figure 4) can be explained by the higher mobility of Ag^+ ions that, during the RESET process, is responsible for the creation of a larger gap in the conductive filament and, thus, a higher HRS. In a similar fashion, the lower mobility of Ag^+ ions in absence of moisture is responsible for the formation of an unstable conductive path giving rise to volatile switching, as observed in vacuum for sputtered ZnO films.

By comparing the effect of moisture with other ECM cells, it is worth noticing that the influence of moisture on the forming voltage results to be less pronounced in case of ZnO-based devices compered to SiO_2- and Ta_2O_5-based ECM cells, where switching in absence of moisture was reported to be not observable.[7] Also, the dependence of the SET voltage on humidity is in accordance with observations reported in case of SiO_2, where the dependence of operating voltages on the humidity level was ascribed to the desorption of water molecules in the metal-oxide matrix by decreasing the ambient pressure.[8]

Importantly, it is worth noticing that the influence of moisture on ZnO resistive switching properties is more pronounced for RF sputtered films, where the smaller grain size resulted in a larger number of grain boundaries and, thus, in higher level of moisture adsorption and an increased amount of possible pathways for ion migration. Last, it is important to remark that prolonged exposure to water molecules can be responsible for device damaging because of degradation and corrosion of ZnO.[50]

4. Conclusion

In this work, the structural-dependent effect of moisture on resistive switching behavior of electrochemical metallization

© 2021 The Authors. Advanced Materials Interfaces published by Wiley-VCH GmbH

memory cells based on ZnO thin films was experimentally investigated. Moisture adsorbed at grain boundaries was found to modify the electrical resistance of ZnO thin films by altering the electronic conduction mechanism and by providing additional ionic species. Moreover, the influence of moisture on dissolution and migration of ionic species (Ag^+) underlying resistive switching events tunes resistive switching characteristics. In particular, it was observed that the presence of moisture is responsible for a decrease of forming and SET voltages and leads to an increase of the ON/OFF ratio. Different structural properties of the ZnO thin films result in a more evident H_2O influence in case of sputtered ZnO films where the smaller grain size and the increased number of grain boundaries facilitate moisture adsorption. These results highlight the importance of controlling structural properties of metal oxides for a rational design of resistive switching devices.

5. Experimental Section

Resistive Switching ZnO Thin Film Devices: ZnO thin films were realized by CVD and sputtering as reported in a previous work.[43] Both ZnO films were realized on Pt thin film realized sputtering (Kurt J. Lesker, PVD 75) on a commercial SiO_2/Si commercial wafer by exploiting a Ta adhesion layer. Chemical vapor deposited ZnO films were realized by means of low pressure chemical vapor deposition (LP-CVD). The process was performed at low pressure in a horizontal quartz tubular furnace by placing the Pt substrate on an alumina boat at 650 °C for 20 min, flushing Ar as carrier gas (300 sccm), O_2 as gas precursor (150 sccm), and by using a Zn foil (purity 99.99%) as the Zn source. The measured pressure during the growth process was 1.3 Torr. Sputtered ZnO films were grown on the Pt substrate by RF magnetron sputtering (frequency of 13.56 MHz) with a 4-in. diameter ceramic ZnO target. The process was performed at room temperature in a pure Ar atmosphere (Ar flow of 40 sccm, gas pressure of 5×10^{-3} Torr) with a deposition time of 4 min. The target-to-substrate distance was about 8 cm and the RF power was 100 W. 15 min of pre-sputtering were performed before starting the deposition to clean the ZnO target avoiding incorporation of contaminants during the film growth. Resistive switching devices based on ZnO thin films were realized by exploiting the Pt growth substrate with thickness of 100 nm as bottom electrode and by realizing $\approx 50 \times 50$ µm Ag top electrodes with thickness of 100 nm.

Atmosphere-Controlled Measurements: Electrical characterization of devices was performed in a custom realized probe station equipped with a chamber connected to a vacuum system where it is possible to control and measure the humidity level. Measurements performed in a controlled humidity environment were performed by controlling the chamber humidity content by flushing N_2 in a cascade of gas wash bottles filled with deionized water. Before filling the chamber with the desired gas composition, the chamber was evacuated down to $\approx 10^{-5}$ mbar. During measurements, the RH was measured by means of a humidity sensor placed into the chamber. Electrical measurements were performed with a Keithley 6430 sub-femto sourcemeter with remote preamplifier, Keithley 2636A and Keithley 2634B. In box plots, midlines represent the median value, open square the mean value, boxes the 25th and 75th percentiles, whiskers the 10th and 90th percentiles while crosses the maximum and minimum values.

Supporting Information

Supporting Information is available from the Wiley Online Library or from the author.

Acknowledgements

Part of this work was supported by the European project MEMQuD, code 20FUN06. This project (EMPIR 20FUN06 MEMQuD) received funding from the EMPIR programme co-financed by the participating states and from the European Union's Horizon 2020 research and innovation programme. The support by Mauro Raimondo in helping with SEM measurements, by Daliborka Erdoglija for helping with device fabrication, and by Thomas Poessinger for helping with graphics is gratefully acknowledged.

Conflict of Interest

The authors declare no conflict of interest.

Data Availability Statement

The dataset of this work is available in Zenodo https://doi.org/10.5281/zenodo.5095263.

Keywords

effect of moisture on electroforming, electrical conductivity, memristors, nanostructures, resistive switching

Received: June 3, 2021
Revised: July 1, 2021
Published online: July 28, 2021

[1] J. J. Yang, D. B. Strukov, D. R. Stewart, *Nat. Nanotechnol.* **2013**, *8*, 13.
[2] Q. Xia, J. J. Yang, *Nat. Mater.* **2019**, *18*, 309.
[3] Z. Wang, H. Wu, G. W. Burr, C. S. Hwang, K. L. Wang, Q. Xia, J. J. Yang, *Nat. Rev. Mater.* **2020**, *5*, 173.
[4] T. Shi, R. Wang, Z. Wu, Y. Sun, J. An, Q. Liu, *Small Struct.* **2021**, *2*, 2000109.
[5] R. Waser, R. Dittmann, G. Staikov, K. Szot, *Adv. Mater.* **2009**, *21*, 2632.
[6] I. Valov, R. Waser, J. R. Jameson, M. N. Kozicki, *Nanotechnology* **2011**, *22*, 289502.
[7] I. Valov, T. Tsuruoka, *J. Phys. D: Appl. Phys.* **2018**, *51*, 413001.
[8] T. Tsuruoka, K. Terabe, T. Hasegawa, I. Valov, R. Waser, M. Aono, *Adv. Funct. Mater.* **2012**, *22*, 70.
[9] F. Messerschmitt, M. Kubicek, J. L. M. Rupp, *Adv. Funct. Mater.* **2015**, *25*, 5117.
[10] Y. Tao, Z. Wang, H. Xu, W. Ding, X. Zhao, Y. Lin, Y. Liu, *Nano Energy* **2020**, *71*, 104628.
[11] G. Zhou, Z. Ren, B. Sun, J. Wu, Z. Zou, S. Zheng, L. Wang, S. Duan, Q. Song, *Nano Energy* **2020**, *68*, 104386.
[12] K.-H. Son, K.-M. Kang, H.-H. Park, H.-S. Lee, *Phys. Status Solidi* **2020**, 2000702.
[13] G. Zhou, B. Sun, Z. Ren, L. Wang, C. Xu, B. Wu, P. Li, Y. Yao, S. Duan, *Chem. Commun.* **2019**, *55*, 9915.
[14] A. Younis, D. Chu, A. H. Shah, H. Du, S. Li, *ACS Appl. Mater. Interfaces* **2017**, *9*, 1585.
[15] S. Tappertzhofen, I. Valov, T. Tsuruoka, T. Hasegawa, R. Waser, M. Aono, *ACS Nano* **2013**, *7*, 6396.
[16] M. Lübben, S. Wiefels, R. Waser, I. Valov, *Adv. Electron. Mater.* **2018**, *4*, 1700458.
[17] T. Tsuruoka, T. Hasegawa, K. Terabe, M. Aono, *J. Electroceram.* **2017**, *39*, 143.

© 2021 The Authors. Advanced Materials Interfaces published by Wiley-VCH GmbH

[18] H. Yang, S. Cai, D. Wu, X. Fang, *Adv. Electron. Mater.* **2020**, *6*, 2000659.
[19] A. Janotti, C. G. Van de Walle, *Rep. Prog. Phys.* **2009**, *72*, 126501.
[20] J. Theerthagiri, S. Salla, R. A. Senthil, P. Nithyadharseni, A. Madankumar, P. Arunachalam, T. Maiyalagan, H.-S. Kim, *Nanotechnology* **2019**, *30*, 392001.
[21] P. Zhang, J. Wu, T. Zhang, Y. Wang, D. Liu, H. Chen, L. Ji, C. Liu, W. Ahmad, Z. D. Chen, S. Li, *Adv. Mater.* **2018**, *30*, 1703737.
[22] J. Liu, Y. Wang, J. Ma, Y. Peng, A. Wang, *J. Alloys Compd.* **2019**, *783*, 898.
[23] B. Zhao, F. Wang, H. Chen, L. Zheng, L. Su, D. Zhao, X. Fang, *Adv. Funct. Mater.* **2017**, *27*, 1700264.
[24] Y. Ning, Z. Zhang, F. Teng, X. Fang, *Small* **2018**, *14*, 1703754.
[25] W. Gao, Z. Li, *Int. J. Nanotechnol.* **2009**, *6*, 245.
[26] Z. L. Wang, *J. Phys. Condens. Matter* **2004**, *16*, R829.
[27] G. Milano, S. Porro, I. Valov, C. Ricciardi, *Adv. Electron. Mater.* **2019**, *5*, 1800909.
[28] G. Milano, M. Luebben, Z. Ma, R. Dunin-Borkowski, L. Boarino, C. F. Pirri, R. Waser, C. Ricciardi, I. Valov, *Nat. Commun.* **2018**, *9*, 5151.
[29] G. Milano, S. Porro, M. Y. Ali, K. Bejtka, S. Bianco, F. Beccaria, A. Chiolerio, C. F. Pirri, C. Ricciardi, *J. Phys. Chem. C* **2018**, *122*, 866.
[30] J. Qi, M. Olmedo, J. Ren, N. Zhan, J. Zhao, J.-G. Zheng, J. Liu, *ACS Nano* **2012**, *6*, 1051.
[31] F. M. Simanjuntak, D. Panda, K.-H. Wei, T.-Y. Tseng, *Nanoscale Res. Lett.* **2016**, *11*, 368.
[32] M. Laurenti, S. Porro, C. F. Pirri, C. Ricciardi, A. Chiolerio, *Crit. Rev. Solid State Mater. Sci.* **2017**, *42*, 153.
[33] D. Conti, M. Laurenti, S. Porro, C. Giovinazzo, S. Bianco, V. Fra, A. Chiolerio, C. F. Pirri, G. Milano, C. Ricciardi, *Nanotechnology* **2019**, *30*, 065707.
[34] F. M. Simanjuntak, T. Ohno, S. Samukawa, *ACS Appl. Electron. Mater.* **2019**, *1*, 18.
[35] F. Messerschmitt, M. Jansen, J. L. M. Rupp, *Adv. Electron. Mater.* **2018**, *4*, 1800282.
[36] F. M. Simanjuntak, O. K. Prasad, D. Panda, C.-A. Lin, T.-L. Tsai, K.-H. Wei, T.-Y. Tseng, *Appl. Phys. Lett.* **2016**, *108*, 183506.
[37] F. M. Simanjuntak, T. Ohno, S. Samukawa, *AIP Adv.* **2019**, *9*, 105216.
[38] F. M. Simanjuntak, T. Ohno, S. Samukawa, *ACS Appl. Electron. Mater.* **2019**, *1*, 2184.
[39] F. M. Simanjuntak, T. Ohno, S. Chandrasekaran, T.-Y. Tseng, S. Samukawa, *Nanotechnology* **2020**, *31*, 26LT01.
[40] A. H. N. Melo, M. A. Macêdo, *PLoS One* **2016**, *11*, e0168515.
[41] C. Hu, Q. Wang, S. Bai, M. Xu, D. He, D. Lyu, J. Qi, *Appl. Phys. Lett.* **2017**, *110*, 073501.
[42] T.-H. Huang, P.-K. Yang, D.-H. Lien, C.-F. Kang, M.-L. Tsai, Y.-L. Chueh, J.-H. He, *Sci. Rep.* **2015**, *4*, 4402.
[43] G. Milano, M. Luebben, M. Laurenti, S. Porro, K. Bejtka, S. Bianco, U. Breuer, L. Boarino, I. Valov, C. Ricciardi, *Adv. Mater. Interfaces* **2019**, *6*, 1900803.
[44] F. Zhuge, S. Peng, C. He, X. Zhu, X. Chen, Y. Liu, R.-W. Li, *Nanotechnology* **2011**, *22*, 275204.
[45] K. Bejtka, G. Milano, C. Ricciardi, C. F. Pirri, S. Porro, *ACS Appl. Mater. Interfaces* **2020**, *12*, 29451.
[46] M. Lübben, S. Menzel, S. G. Park, M. Yang, R. Waser, I. Valov, *Nanotechnology* **2017**, *28*, 135205.
[47] I. Valov, W. D. Lu, *Nanoscale* **2016**, *8*, 13828.
[48] K. Liu, L. Qin, X. Zhang, J. Zhu, X. Sun, K. Yang, Y. Cai, Y. Yang, R. Huang, *Faraday Discuss.* **2019**, *213*, 41.
[49] G. Milano, F. Raffone, M. Luebben, L. Boarino, G. Cicero, I. Valov, C. Ricciardi, *ACS Appl. Mater. Interfaces* **2020**, *12*, 48773.
[50] G. Milano, L. D'Ortenzi, K. Bejtka, L. Mandrile, A. M. Giovannozzi, L. Boarino, C. F. Pirri, C. Ricciardi, S. Porro, *J. Phys. Chem. C* **2018**, *122*, 8011.

© 2021 The Authors. Advanced Materials Interfaces published by Wiley-VCH GmbH